JACS
JOURNAL OF THE AMERICAN CHEMICAL SOCIETY

Subscriber access provided by ISTANBUL TEKNIK UNIV

Article

Passivation of GaAs Nanocrystals by Chemical Functionalization

Matthew C. Traub, Julie S. Biteen, Bruce S. Brunschwig, and Nathan S. Lewis

J. Am. Chem. Soc., **2008**, 130 (3), 955-964 • DOI: 10.1021/ja076034p

Downloaded from http://pubs.acs.org on February 8, 2009

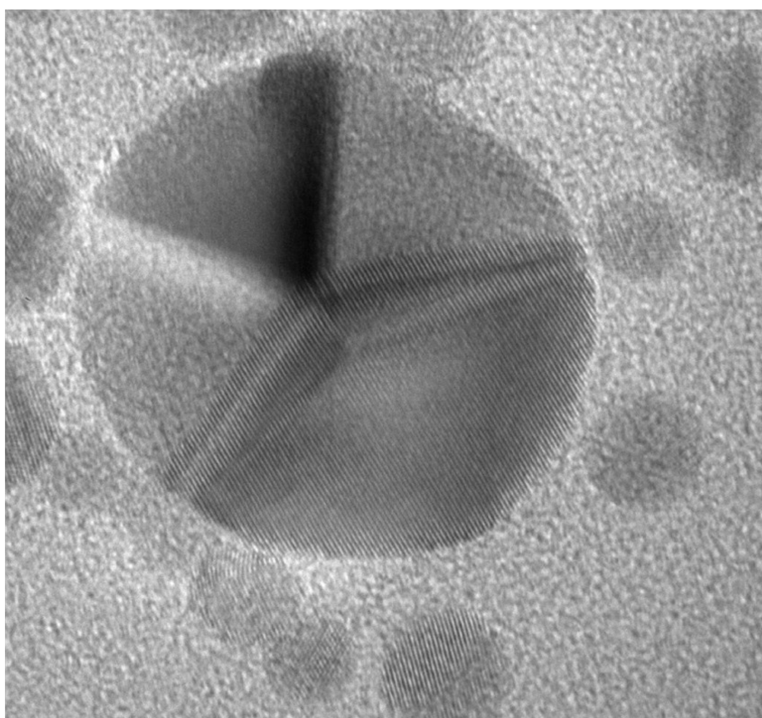

More About This Article

Additional resources and features associated with this article are available within the HTML version:

- Supporting Information
- Links to the 1 articles that cite this article, as of the time of this article download
- Access to high resolution figures
- Links to articles and content related to this article
- Copyright permission to reproduce figures and/or text from this article

View the Full Text HTML

ACS Publications
High quality. High impact.

Journal of the American Chemical Society is published by the American Chemical Society. 1155 Sixteenth Street N.W., Washington, DC 20036

J|A|C|S
ARTICLES
Published on Web 01/03/2008

Passivation of GaAs Nanocrystals by Chemical Functionalization

Matthew C. Traub, Julie S. Biteen, Bruce S. Brunschwig,* and Nathan S. Lewis*

Division of Chemistry and Chemical Engineering, 210 Noyes Laboratory, 127-72, Beckman Institute and Kavli Nanoscience Institute, California Institute of Technology, 1200 E. California Boulevard, Pasadena, California 91125

Received August 10, 2007; E-mail: bsb@caltech.edu; nslewis@caltech.edu

Abstract: The effective use of nanocrystalline semiconductors requires control of the chemical and electrical properties of their surfaces. We describe herein a chemical functionalization procedure to passivate surface states on GaAs nanocrystals. Cl-terminated GaAs nanocrystals have been produced by anisotropic etching of oxide-covered GaAs nanocrystals with 6 M HCl(aq). The Cl-terminated GaAs nanocrystals were then functionalized by reaction with hydrazine or sodium hydrosulfide. X-ray photoelectron spectroscopic measurements revealed that the surfaces of the Cl-, hydrazine-, and sulfide-treated nanocrystals were As-rich, due to significant amounts of As^0. However, no As^0 was observed in the photoelectron spectra after the hydrazine-terminated nanocrystals were annealed at 350° C under vacuum. After the anneal, the N 1s peak of hydrazine-exposed GaAs nanocrystals shifted to 3.2 eV lower binding energy. This shift was accompanied by the appearance of a Ga 3d peak shifted 1.4 eV from the bulk value, consistent with the hypothesis that a gallium oxynitride capping layer had been formed on the nanocrystals during the annealing process. The band gap photoluminescence (PL) was weak from the Cl- and hydrazine- or sulfide-terminated nanocrystals, but the annealed nanocrystals displayed strongly enhanced band-edge PL, indicating that the surface states of GaAs nanocrystals were effectively passivated by this two-step, wet chemical treatment.

1. Introduction

GaAs is one of the most important semiconductors in modern electronics.[1] Specifically, GaAs has been used as the absorber layer in some of the most efficient solar cells constructed to date.[2] Unlike Si, for which the H-terminated Si(111) surface and Si/SiO_2 interfaces are highly passivated electrically, most devices that use GaAs require the presence of epitaxial capping layers, such as $Al_xGa_{1-x}As$, to minimize the effects of electrical trap states at the GaAs surface. While these methods yield extremely low recombination velocities at single-crystal GaAs/$Al_xGa_{1-x}As$ interfaces,[3,4] they are not well suited to more heterogeneous structures, particularly solution-grown GaAs nanocrystals or nanowires. For these types of structures, a set of versatile solution passivation chemistry techniques would be quite valuable.

Several different wet chemical procedures have been shown to provide some degree of electrical passivation of bulk GaAs surfaces. Sulfide- and thiol-based treatments have been shown to improve the electrical properties of GaAs surfaces.[5−7] More recently, hydrazine treatments of GaAs(100) have been reported to be more effective than sulfide treatments at increasing the photoluminescence (PL) intensity of GaAs in contact with air.[8] To our best knowledge, this chemistry has not previously been explored on nanocrystalline GaAs surfaces.

Chemically synthesized GaAs nanocrystals provide potential advantages over bulk single-crystal GaAs, in terms of both cost and the ability to exploit quantum confinement effects. GaAs nanocrystals are however much less thoroughly studied than their various II−VI counterparts.[9,10] Several procedures have been reported for the synthesis of GaAs nanocrystals,[11,12] many of which involve the reaction of an As precursor with $GaCl_3$. The reaction is performed in a coordinating solvent that caps the nanocrystals and controls their growth.[13,14] Unlike CdSe nanocrystals, for which core−shell structures have been developed to passivate the interface states and yield intense band gap PL,[15,16] no such method has been reported to date for GaAs. A general set of methods for the chemical functionalization and

(1) Sze, S. M. *The Physics of Semiconductor Devices*, 2nd ed.; John Wiley & Sons: New York, 1981.
(2) Green, M. A.; Emery, K.; King, D. L.; Igari, S.; Warta, W. *Prog. Photovoltaics* **2003**, *11*, 347.
(3) Nelson, R. J. *J. Vac. Sci. Technol.* **1978**, *15*, 1475.
(4) Nelson, R. J.; Sobers, R. G. *Appl. Phys. Lett.* **1978**, *32*, 761.
(5) Skromme, B. J.; Sandroff, C. J.; Yablonovitch, E.; Gmitter, T. *Appl. Phys. Lett.* **1987**, *51*, 2022.
(6) Sandroff, C. J.; Nottenburg, R. N.; Bischoff, J. C.; Bhat, R. *Appl. Phys. Lett.* **1987**, *51*, 33.
(7) Lunt, S. R.; Santangelo, P. G.; Lewis, N. S. *J. Vac. Sci. Technol., B* **1991**, *9*, 2333.
(8) Berkovits, V. L.; Ulin, V. P.; Losurdo, M.; Capezzuto, P.; Bruno, G.; Perna, G.; Capozzi, V. *Appl. Phys. Lett.* **2002**, *80*, 3739.
(9) Esteves, A. C. C.; Trindade, T. *Curr. Opin. Solid State Mater. Sci.* **2002**, *6*, 347.
(10) Masala, O.; Seshadri, R. *Ann. Rev. Mat. Res.* **2004**, *34*, 41.
(11) Salata, O. V.; Dobson, P. J.; Hull, P. J.; Hutchison, J. L. *Appl. Phys. Lett.* **1994**, *65*, 189.
(12) Sercel, P. C.; Saunders, W. A.; Atwater, H. A.; Vahala, K. J.; Flagan, R. C. *Appl. Phys. Lett.* **1992**, *61*, 696.
(13) Malik, M. A.; O'Brien, P.; Norager, S.; Smith, J. *J. Mater. Chem.* **2003**, *13*, 2591.
(14) Uchida, H.; Curtis, C. J.; Nozik, A. J. *J. Phys. Chem.* **1991**, *95*, 5382.
(15) Dabbousi, B. O.; RodriguezViejo, J.; Mikulec, F. V.; Heine, J. R.; Mattoussi, H.; Ober, R.; Jensen, K. F.; Bawendi, M. G. *J. Phys. Chem. B* **1997**, *101*, 9463.

10.1021/ja076034p CCC: $40.75 © 2008 American Chemical Society

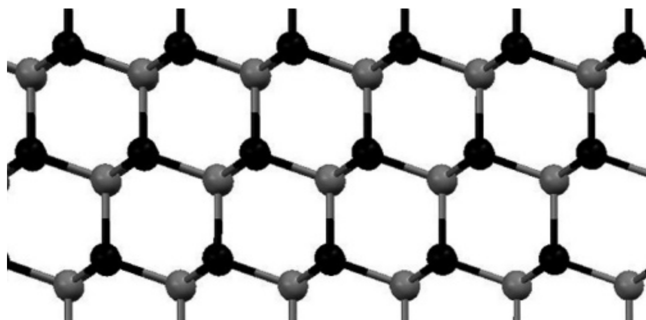

Figure 1. Cross-sectional structure of GaAs and its (111) surfaces. Dark atoms represent Ga, and light atoms represent As. The (111)A face at the top of the image has Ga dangling bonds normal to the surface plane, while (111)B face at the bottom of the image has As dangling bonds normal to the surface plane.

passivation of GaAs nanocrystals is an important step for the widespread use of these materials in both fundamental studies and in optical and electronic devices.

We describe a method for passivating GaAs nanocrystals that produces strongly enhanced band gap PL emission. Etching native oxide-terminated single-crystal GaAs(111)A surfaces with a 6 M HCl(aq) solution has been shown to produce highly ordered,[17,18] oxide-free[19] Cl-terminated surfaces. Furthermore, of all low index GaAs surfaces, the (111)A face, shown in Figure 1, is known to have the slowest etch rate in contact with oxidizing etches.[20] Thus, we reasoned that treating as-synthesized, oxide-capped GaAs nanocrystals[21] with 6 M HCl(aq) would cleanly remove the oxide layer and anisotropically etch the nanocrystals, predominantly producing surfaces terminated by Ga−Cl bonds. We demonstrate that this procedure indeed is applicable to GaAs nanocrystal surfaces. Furthermore, we demonstrate that the surface-bound Cl can be displaced by wet chemical reactions to introduce other functional groups onto the GaAs surface. This two-step functionalization procedure is not restricted to bulky groups chosen to limit the growth of the nanocrystals and allows for a significant degree of control over the chemistry of the resulting capped GaAs nanocrystal surfaces. Importantly, such functionalized GaAs nanocrystals show intense band gap PL, indicating that the electrical trap density has been significantly reduced on their surfaces and therefore possibly enabling the use of GaAs nanocrystals for spectroscopic investigations and electronic device applications similar to those that have been developed for core−shell capped II−IV nanoparticles.[22−24]

2. Experimental Section

2.1. Materials and Methods. Arsenic powder (ESPI, 99.9999%), ultra-dry $GaCl_3$ (Alfa, 99.9999%), and 44:56 Na/K alloy (Strem) were used as received. Toluene (Aldrich) and bis(2-methoxy ethyl) ether (diglyme) (Alfa) were distilled over Na and degassed before use. Concentrated (12 M) HCl(aq) (Baker), concentrated N_2H_4(aq) (Aldrich, 35 wt %), and sodium hydrosulfide hydrate ($NaSH \cdot xH_2O$) were used as received. Hydrazine-d_4 monohydrate-d_2 (Aldrich) was diluted with D_2O (Aldrich) to give a 35% by weight solution. H_2O with a resistivity > 17.8 MΩ cm^{-1}, obtained from a Barnsted Nanopure system, was used at all times.

GaAs nanocrystals were synthesized according to the method of Kher and Wells.[21] First, 0.56 g of NaK alloy and 0.51 g of As (9% excess) were suspended in toluene and refluxed under flowing ultrahigh purity Ar for 2 days, to yield $(Na/K)_3As$. This black suspension was cooled to 0 °C, and 1.17 g of $GaCl_3$ dissolved in either toluene or bis(2-methoxy ethyl) ether was then added. This mixture was refluxed for an additional 2 days under Ar. The solution was then cooled to room temperature, and ~70 mL of H_2O were added. After 30 min of stirring under Ar, the black suspension was opened to air, filtered, and rinsed with water. The collected dark gray solids were heated to 350 °C under vacuum to remove excess As. Alternatively, when the reaction was complete, ~70 mL of CH_3OH were added. After 30 min of stirring, the suspension was then allowed to settle for 24 h. The supernatant solution was removed, ~300 mL of CH_3OH were added, and the solution was allowed to settle for another 24 h. The supernatant was then removed, and the black solids were collected by centrifugation. These solids were rinsed with CH_3OH, dried *in vacuo*, and heated to 350 °C under vacuum to remove excess As.

To Cl-terminate the surfaces, the synthesized GaAs nanoparticles were sonicated in a 6 M HCl(aq) solution for 40 min and the suspension was then centrifuged. The etching solution was removed with a pipet, and the collected particles were rinsed with fresh etching solution. The particles were sonicated in a fresh etching solution for another 5 min and then centrifuged again. The 6 M HCl(aq) solution was removed, and the particles were then collected.

Hydrazine functionalization reactions were performed by sonicating the etched GaAs nanocrystals for 30 min in a concentrated (≈17 M) aqueous hydrazine solution and allowing the particles to settle at ambient temperature for an additional 2 h. The suspension was centrifuged, and the supernatant was removed. The particles were then rinsed and centrifuged with water or acetone. Once dispersed in acetone, the solids could not all be collected by centrifugation, and the acetone rinses retained a reddish-brown color, suggesting a significantly higher solubility for the functionalized particles. This solution displayed an absorption peak at ~480 nm but was not subjected to further analysis.

Functionalization with NaSH was performed by the same method as that for hydrazine except that a 1 M NaSH(aq) solution was used instead of the hydrazine solution. As with the hydrazine-treated particles, some fraction of the NaSH-treated GaAs nanoparticles could not be collected by centrifugation, leaving a reddish-brown supernatant.

2.2. Instrumentation. TEM images were obtained on a Philips EM430 300 kV microscope, whereas powder X-ray diffraction (XRD) data were collected using a Philips X'Pert Pro diffractometer with a Cu anode X-ray source. Samples for XRD were dispersed onto a "zero-background" Si substrate.

X-ray photoelectron spectroscopy (XPS) was performed using a Surface Science M-Probe system.[25,26] Samples were dispersed on degreased, conductive Si substrates, inserted via a quick-entry load lock into the ultrahigh vacuum (UHV) chamber, and kept at a base pressure of $\leq 1 \times 10^{-9}$ Torr. For these experiments, 1486.6 eV X-rays generated from an Al Kα source illuminated the sample at an incident angle of 35° off of the surface. Photoelectrons emitted along a trajectory 35° off of the surface were collected by a hemispherical analyzer. The vertical planes of the source and analyzer were at right angles to each other. For the oxide-terminated GaAs nanoparticles, an 8711 Charge Neutralizer electron flood gun (Surface Science Instruments) was used to compensate the charging effects. On each sample, a "survey" scan

(16) Peng, X. G.; Schlamp, M. C.; Kadavanich, A. V.; Alivisatos, A. P. *J. Am. Chem. Soc.* **1997**, *119*, 7019.
(17) Lu, Z. H.; Chatenoud, F.; Dion, M. M.; Graham, M. J.; Ruda, H. E.; Koutzarov, I.; Liu, Q.; Mitchell, C. E. J.; Hill, I. G.; McLean, A. B. *Appl. Phys. Lett.* **1995**, *67*, 670.
(18) Lu, Z. H.; Tyliszczak, T.; Hitchcock, A. P. *Phys. Rev. B* **1998**, *58*, 13820.
(19) Traub, M. C.; Biteen, J. S.; Michalak, D. J.; Webb, L. J.; Brunschwig, B. S.; Lewis, N. S. *J. Phys. Chem. B* **2006**, *110*, 15641.
(20) Tarui, Y.; Komiya, Y.; Harada, Y. *J. Electrochem. Soc.* **1971**, *118*, 118.
(21) Kher, S. S.; Wells, R. L. *Chem. Mater.* **1994**, *6*, 2056.
(22) Eisler, H. J.; Sundar, V. C.; Bawendi, M. G.; Walsh, M.; Smith, H. I.; Klimov, V. *Appl. Phys. Lett.* **2002**, *80*, 4614.
(23) Colvin, V. L.; Schlamp, M. C.; Alivisatos, A. P. *Nature* **1994**, *370*, 354.
(24) Afzaal, M.; O'Brien, P. *J. Mater. Chem.* **2006**, *16*, 1597.
(25) Bansal, A.; Li, X. L.; Yi, S. I.; Weinberg, W. H.; Lewis, N. S. *J. Phys. Chem. B* **2001**, *105*, 10266.
(26) Webb, L. J.; Lewis, N. S. *J. Phys. Chem. B* **2003**, *107*, 5404.

of core photoelectron binding energies from 1 to 1200 binding eV was collected to identify the chemical species present on the surface. Higher resolution data were collected for the atoms of interest.

Energies deduced from all of the XPS measurements are reported herein as binding energies in eV. All binding energies are referenced to the bulk (Ga)As $3d_{5/2}$ peak at 41.1 eV. Before fitting the data, a Shirley background was calculated and subtracted from the original spectra.[27−29] In accord with reported procedures, the As 3d spectra were fitted to a series of 80% Gaussian/20% Lorentzian Voigt-function doublets to account for the $3d_{5/2}$ and $3d_{3/2}$ spin−orbit components of each peak. The peaks that comprised each doublet were mutually constrained to have the same peak width, to be separated by 0.7 eV, and to have an area ratio of (3:2).[30] Peak widths for the bulk and elemental As peaks were typically ~1 eV. Because the separation between the $3d_{5/2}$ and $3d_{3/2}$ spin−orbit components of the Ga 3d peak (0.44 eV)[30] is significantly less than the resolution of our spectrometer, the Ga 3d signals were fit as single peaks.

Diffuse reflectance infrared (IR) spectra were collected with a Vertex 70 Fourier transform IR (Bruker Optics) using a Seagull variable-angle reflectance (Harrick Scientific) attachment. The sample chamber was continually purged with N_2(g) during data collection. Samples were dispersed on degreased stainless steel plates. Data were collected from 4000 cm^{-1} to 500 cm^{-1} at 2 cm^{-1} resolution for angles between 15 and 60 degrees, for which the strongest signals were observed. 256 scans were taken for each sample, with background scans of the sample plate subtracted from each spectrum. Reflectance spectra were Kubelka−Munk transformed (KM = $(1-R)^2/2R$), and for samples with stronger light scattering, a scattering background was subtracted.

Photoluminescence (PL) measurements were made on particles that were dispersed in optical grade CH_3OH (EMD Chemicals). The particles were then either loaded into quartz cuvettes or were deposited as films on Si substrates. The particles were excited with an Ar ion laser operating at 488 or 514 nm at an output power density of 300 mW mm^{-2}. No differences in PL behavior were observed between spectra collected at these different excitation wavelengths. The PL signals were collected from the front face of the Si substrate or the cuvette with a Princeton Instruments Spec-10 Si charge-coupled device (CCD) detector (sensitivity range 200−1100 nm) cooled with liquid N_2 to −132 °C, in conjunction with a 27.5-cm focal length Oriel MS257 grating spectrograph. A 550-nm long-pass filter in front of the entrance slit was used to cut off scattered laser illumination.

3. Results and Discussion

3.1. Characterization of As-Synthesized, Oxide-Coated GaAs Nanocrystals. 3.1.1. X-ray Diffraction. Figure 2 shows the powder X-ray diffraction pattern for the toluene synthesized, oxide-capped GaAs nanocrystals. The most prominent peaks were ascribable to reflections from the GaAs lattice planes. Two broad peaks were also clearly observed, indicative of the presence of some amorphous Ga_2O_3.

The average diameter, L, of these crystallites was determined through use of the Scherrer equation:[31]

$$L = \frac{K\lambda}{B \cos \theta} \quad (1)$$

In this relationship, K is a structure constant of 0.94, λ is the wavelength of the X-rays, B is the full width at half-maximum

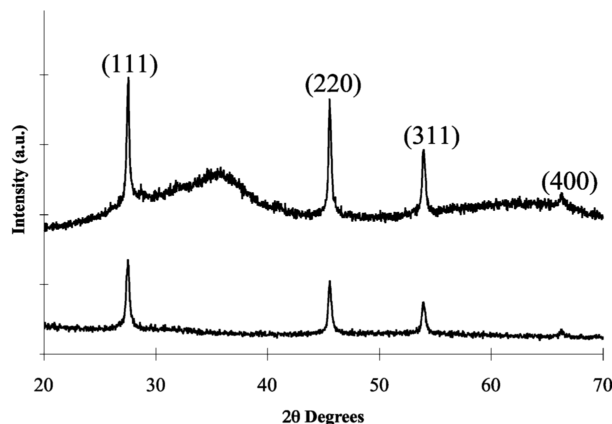

Figure 2. Powder X-ray diffraction pattern of GaAs nanocrystals, synthesized from toluene. The upper diffraction pattern is for the as-synthesized material, while the lower one was measured after HCl(aq) etching. Index labels refer to GaAs lattice reflections, while the broad peaks centered at approximately 35° and 65° in the as-synthesized diffraction pattern correspond to Ga_2O_3.

of the diffraction peak, and θ has its usual meaning. Based on the reflection of the GaAs (111) plane, the crystals had an average diameter of 39 nm, close to the reported value of 36 nm for particles made by this method[21] and well above the calculated quantum confinement limit for GaAs of ~19 nm.[32]

Somewhat smaller (~30 nm) diameter GaAs nanocrystals were produced when the $GaCl_3$ precursor was dissolved in diglyme, rather than toluene. Such nanocrystals were however significantly larger than those obtained previously using nominally the same preparation method.[21,33] GaAs nanoparticles synthesized with diglyme and worked up in CH_3OH were approximately the same size but exhibited significantly less Ga_2O_3 in the XRD data than those synthesized in diglyme and worked up in H_2O.

3.1.2. X-ray Photoelectron Spectroscopy. Due to substantial charging effects, the XPS data on the oxide-capped particles were difficult to interpret quantitatively. Samples for which the use of an electron gun for charge compensation was required exhibited a greatly decreased signal-to-noise ratio relative to more conductive samples. To within the sampling depth of the experiment, the data were completely dominated by signals arising from Ga and As oxides (Figure 3). The surface was significantly enriched in gallium oxides, presumably due to sublimation of As_2O_3 during the purification step and/or due to the higher solubility of As oxides than Ga oxides in aqueous solutions.[34]

3.1.3. Diffuse Reflectance IR Spectra. The diffuse reflectance IR spectra of neat powders of oxide-terminated GaAs nanoparticles exhibited broad peaks observed at 1225, 1040, 825, and 630 cm^{-1} (Figure 4), respectively. For the nanocrystals worked up in CH_3OH rather than H_2O, the band at 825 cm^{-1} was significantly less intense. In accord with previous IR studies of GaAs and its oxides,[35] the bands at 1040 and 825 cm^{-1} can be ascribed to As_2O_3. The band at 1040 cm^{-1} has been observed for the cubic Arsenolite phase of As_2O_3,[36] while the band at

(27) Proctor, A.; Sherwood, P. M. A. *Anal. Chem.* **1982**, *54*, 13.
(28) Shirley, D. A. *Phys. Rev. B* **1972**, *5*, 4709.
(29) Contini, G.; Turchini, S. *Comput. Phys. Commun.* **1996**, *94*, 49.
(30) Eastman, D. E.; Chiang, T. C.; Heimann, P.; Himpsel, F. J. *Phys. Rev. Lett.* **1980**, *45*, 656.
(31) Klug, H. P.; Alexander, L. E. *X-Ray Diffraction Procedures For Polycrystalline and Amorphous Materials*, 2nd ed.; John Wiley & Sons: New York, 1974.
(32) Brus, L. E. *J. Chem. Phys.* **1984**, *80*, 4403.
(33) Hagan, C. R. S.; Kher, S. S.; Halaoui, L. I.; Wells, R. L.; Coury, L. A. *Anal. Chem.* **1995**, *67*, 528.
(34) Kirchner, C.; George, M.; Stein, B.; Parak, W. J.; Gaub, H. E.; Seitz, M. *Adv. Funct. Mater.* **2002**, *12*, 266.
(35) Vilar, M. R.; El, Beghdadi, J.; Debontridder, F.; Artzi, R.; Naaman, R.; Ferraria, A. M.; do Rego, A. M. B. *Surf. Interface Anal.* **2005**, *37*, 673.

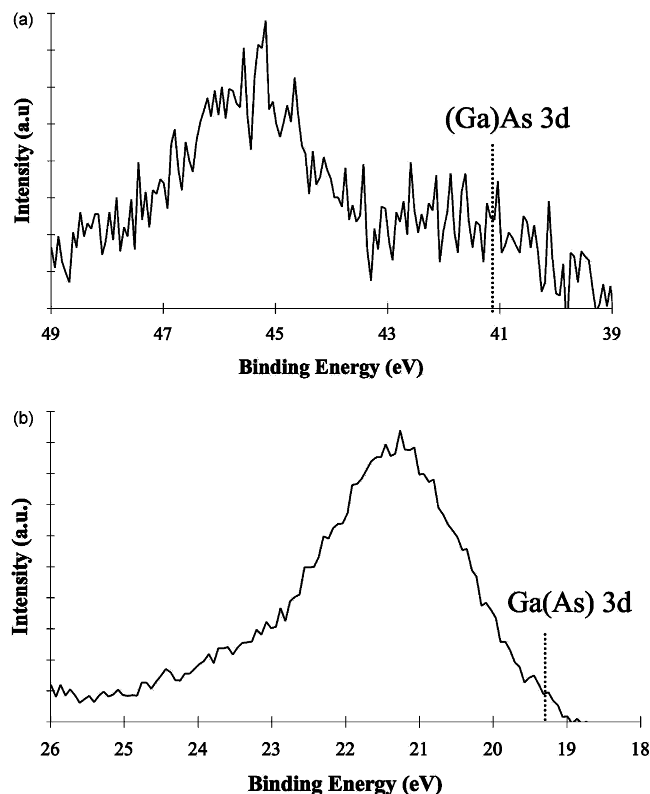

Figure 3. XPS spectra of as-synthesized GaAs nanocrystals from toluene, showing the As 3d (a) and Ga 3d (b) regions. Dotted lines show the expected binding energy of the bulk GaAs peaks.

825 cm^{-1} has been observed for the monoclinic Claudetite phase of As_2O_3.[37] A strong band at 625 cm^{-1} has been observed for amorphous As_2O_3.[36] The GaAs nanocrystal IR data also contained a broad peak at ~3600 cm^{-1} and a weaker peak at ~1600 cm^{-1}, both of which were assigned to surface-bound water.

The XPS results (Figure 3) indicated the presence of significantly more gallium oxides than arsenic oxides, so the IR data would be expected to also exhibit signals ascribable to Ga(III) oxides. No IR signals were observed at the energies reported for powdered[35] or cubic β-Ga_2O_3.[36] The previously observed peaks for amorphous Ga_2O_3[36] are however at 305 and 550 cm^{-1}, outside of the experimentally observable energy range. Consistently, the XRD data (Figure 2) suggest that the native oxide is highly amorphous. We tentatively assign the peak at 1225 cm^{-1} to Ga_2O, a known component of native oxides on GaAs.

3.2. Characterization of HCl(aq)-Etched GaAs Nanocrystals. 3.2.1. X-ray Diffraction. After etching with HCl(aq), only GaAs-based plane reflections, and no signals ascribable to amorphous Ga_2O_3, were present in the XRD pattern (Figure 2) of the GaAs nanoparticles. Line broadening measurements of the etched particles indicated their average diameter had been reduced to ~22 nm. This behavior implies that the crystalline core, as well as the surface oxides, had been etched.

3.2.2. Transmission Electron Microscopy. TEM images revealed the effects of this etching on the morphology of the nanocrystals. The oxide-capped nanocrystals were observed to be roughly spherical (Figure 5a). In contrast, the etching process was anisotropic, and crystal facets were revealed (Figure 5b). The obtained TEM images were not of sufficient resolution to resolve which faces had been revealed. However, studies on single crystals have shown that the (111)A, Ga-rich surface is the face that is most slowly etched under oxidizing conditions.[20] Because other crystal faces are etched away more rapidly, it is likely that the (111)A was preferentially revealed by the 6 M HCl(aq) etch.

3.2.3. X-ray Photoelectron Spectroscopy. 3.2.3.1. Cl 2p Signals. As expected, Cl signals were observed in survey scans of the HCl(aq)-etched GaAs nanocrystals. A detailed scan of the Cl 2p region revealed a doublet, with the Cl $2p_{3/2}$ peak centered at 198.5 eV. The relative intensity of this doublet, compared to the neighboring As 3s peak (205 eV), was much greater than that observed on the Cl-terminated GaAs(111)A surface,[19] as expected for a surface-bound species on a higher

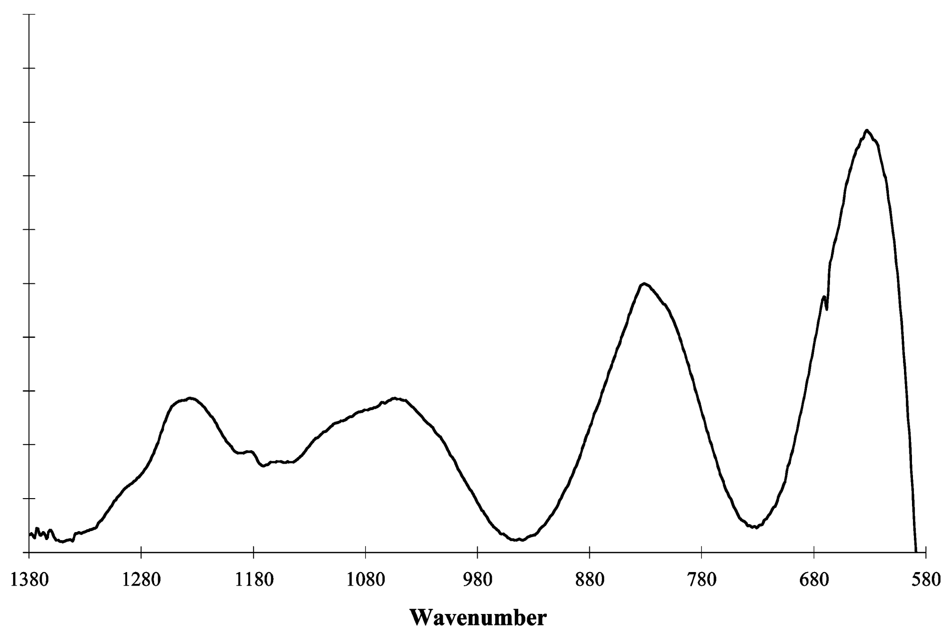

Figure 4. Diffuse reflectance infrared spectrum of as-synthesized GaAs nanocrystals. Peaks at 1040, 825, and 630 cm^{-1} correspond to As_2O_3, while the peak at 1225 cm^{-1} is assigned to Ga_2O.

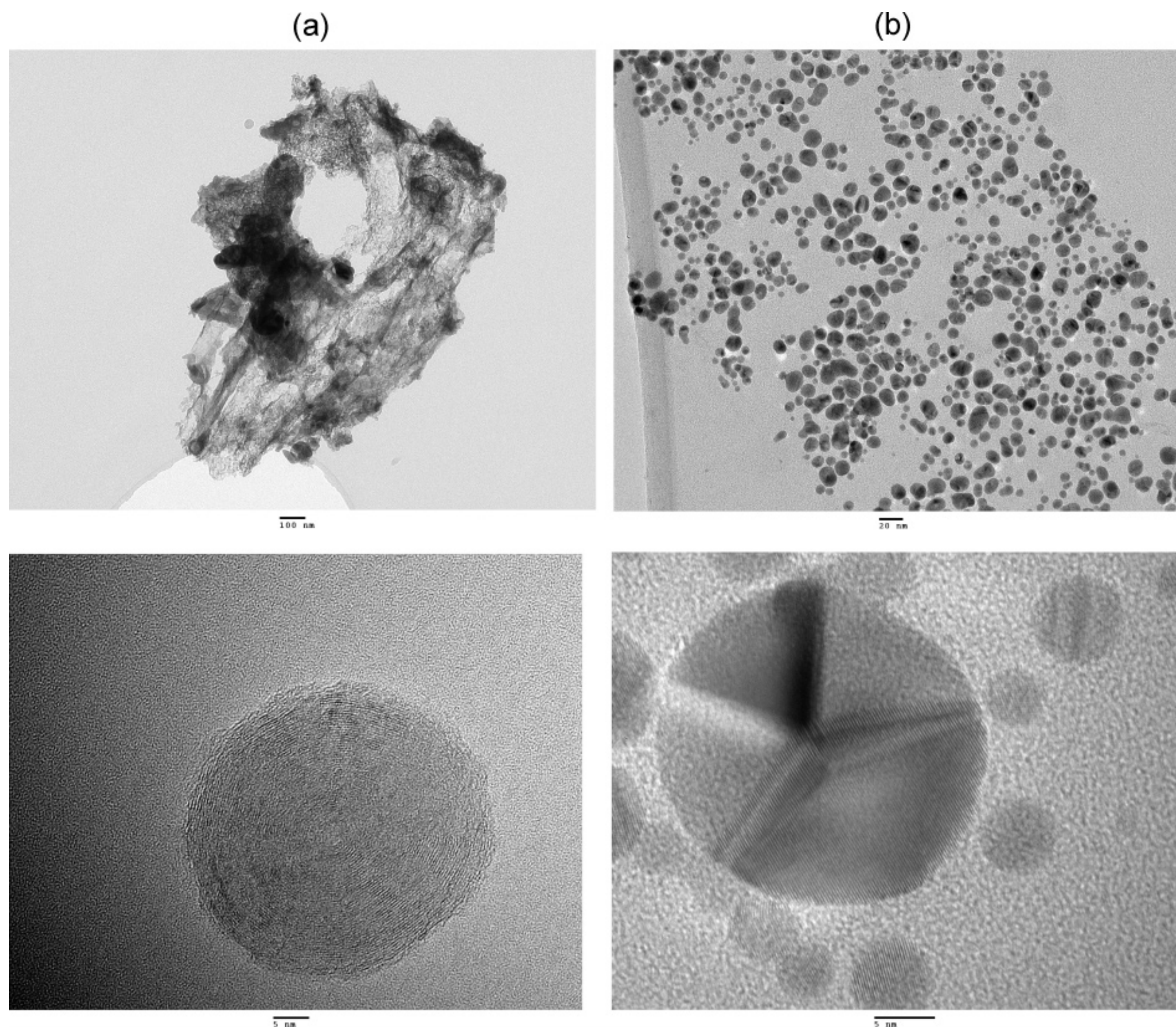

Figure 5. (a) Transmission electron micrographs of oxide-terminated GaAs nanocrystals. (Above) A collection of agglomerated particles. (Below) A single oxide-terminated particle. (b) TEM images of Cl-terminated GaAs nanocrystals. In contrast to the oxide-terminated nanocrystals, the Cl-terminated particles were well-separated, and the beginnings of facet formation could be seen.

surface area sample. When the HCl(aq)-etched GaAs particles were rinsed with water, methanol, or acetone, the Cl signal was not observed, suggesting that the surface Cl-bonds are relatively reactive.

3.2.3.2. As 3d Signals. XPS data for the As 3d region of the HCl(aq)-etched GaAs particles showed the complete removal of As oxides (Figure 6a). The remaining As signal was resolved into two spin−orbit doublets, representing two As chemical species on the surface. The lower energy As $3d_{5/2}$ peak at 41.1 eV is consistent with expectations for bulk GaAs. The As $3d_{5/2}$ peak at 0.6 eV higher binding energy is assigned to elemental As, consistent with previous reports for the binding energy of As^0.[38] A Cl-bonded As surface site might be expected to appear at higher binding energy than the position of the observed signal, as observed for the shift of Cl-bonded Si atoms on the Si(111) surface relative to the bulk.[39] To our knowledge, the binding energy of a Cl-bonded As surface site has not been reported, and it is conceivable that the signal from such a species would overlap with that from As^0. Additionally, for a heterogeneous, nanocrystalline sample, differential charging effects cannot be ruled out. However, as discussed below, the peak at 41.7 eV appears under a variety of different surface conditions, including those for which no Cl is present. Given these observations, it is not likely that Cl-bonded (Ga)As surface sites contribute significantly to this signal.

3.2.3.3. Ga 3d Signals. The Ga 3d region showed the removal of most surface oxides as a result of the 6 M HCl(aq) etching procedure. The Ga 3d signal was well-fitted by two peaks representing separate Ga species (Figure 6b). The larger peak, centered at 19.3 eV, is consistent with expectations for bulk Ga(As), while the smaller peak, at 20.7 eV, is ascribable to Ga_2O_3.[38]

The binding energy of Cl-bonded surface Ga atoms is known to be shifted only 0.35 eV from the bulk Ga 3d peak,[19] a shift significantly less than the energy resolution of the available laboratory XPS instrumentation. Any Ga−Cl surface species are thus expected to appear as part of the bulk peak at 19.3 eV.

Because the particles were deposited on the XPS substrate directly from the aqueous etching solution and dried for several minutes in air, the Ga_2O_3 was presumably formed by reaction with the residual water present during the preparation of the

(36) Palik, E. D.; Ginsburg, N.; Holm, R. T.; Gibson, J. W. *J. Vac. Sci. Technol.* **1978**, *15*, 1488.
(37) Flynn, E. J.; Solin, S. A.; Papatheodorou, G. N. *Phys. Rev. B* **1976**, *13*, 1752.

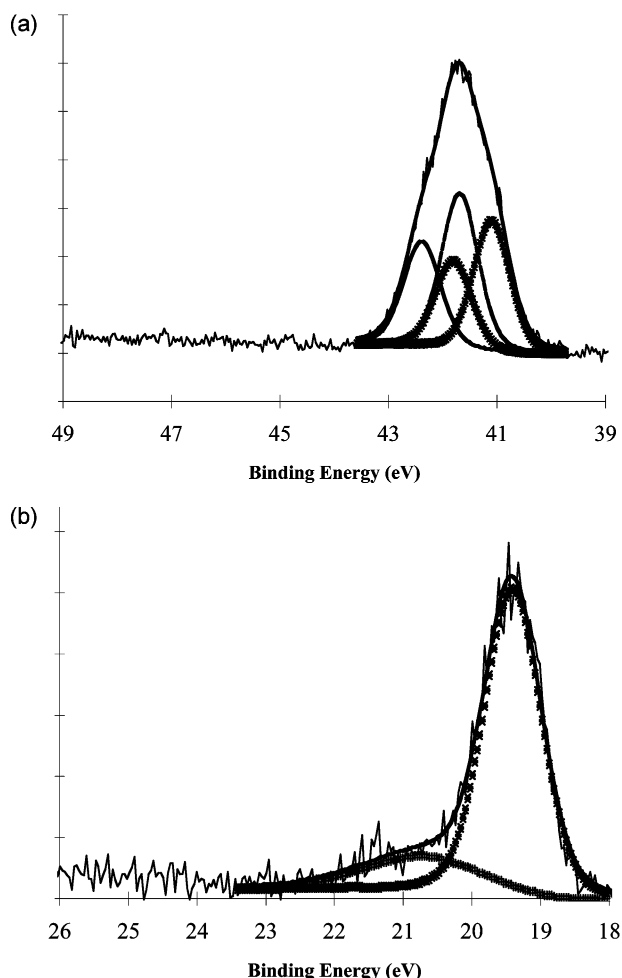

Figure 6. XPS spectra for Cl-terminated GaAs nanocrystals. (a) As 3d region, fit to doublets representing bulk (Ga)As and As^0; (b) Ga 3d region, fit to peaks representing bulk Ga(As) and Ga_2O_3.

samples for the XPS experiments. However, it is possible that a small amount of oxide was not removed during the etching process.

Rinsing the Cl-terminated GaAs particles with a fresh etching solution was necessary before collecting XPS data or performing further functionalization. If the particles were deposited on the Si substrate directly from the original etching solution, another strong peak, centered at ~21.1 eV, was observed in the Ga 3d region of the XPS data. This peak corresponded to $Ga(OH)_3$[19,38] and presumably represented contamination due to Ga hydroxides that were formed during the aqueous etching process.

3.2.3.4. Surface Stoichiometry. Although the equations developed for the determination of overlayer thicknesses on flat surfaces[40] cannot be applied to the nanoparticles, due to surface roughness and shadowing effects,[41,42] the integrated peak areas, corrected for the relevant sensitivity factors σ, can be used to determine the relative elemental abundances within the sample depth probed by XPS at the incident photon energy used in data collection. For the particles synthesized using an aqueous workup, the ratio of the As^0 $3d_{5/2}$ ($\sigma = 1.213$) peak area to the bulk Ga 3d ($\sigma = 1.085$) peak area was 2.4:1, suggesting a significant excess of elemental arsenic on the nanocrystal surfaces.

There are several possible sources of excess As^0 in this material. Some of the As^0 may be formed during the wet etching process. Etching of the native oxides on the GaAs(111)A face with the same HCl(aq) solution has been observed to produce As^0-free surfaces,[19] but this reaction probably does not proceed as cleanly on other GaAs faces or at step edges. Unreacted As starting material may get trapped in the oxide layer during the aqueous workup step, although no As^0 lines were observed in the X-ray diffraction pattern of the oxide-capped particles. Finally, elemental As may be formed at the oxide-GaAs interface during the 350 °C vacuum annealing step of particle purification, through the reaction of GaAs in contact with As_2O_3 to form Ga_2O_3 and As^0.[43]

Use of a methanolic workup in the synthesis of the nanoparticles should result in a much thinner oxide layer during the annealing step and thus produce less As^0. Consistently, a bulk Ga to bulk As ratio of 1.3:1 was observed in the XPS data for such particles. This excess of bulk Ga signal is consistent with an etching mechanism that preferentially reveals Ga-rich faces. As^0 was still observable on this surface, with an As^0 to (Ga)As ratio of 1.2:1. While this represents a substantial reduction in the amount of elemental As present, such levels of As^0 are still sufficient to produce a high density of electrical trap sites, if they are associated with the presence of surficial elemental As.

3.3. Chemical Functionalization of Cl-terminated GaAs Nanocrystals. 3.3.1. Hydrazine-Treated Samples. 3.3.1.1. X-ray Photoelectron Spectroscopy. After treatment with hydrazine, the Cl 2p peak at 198.7 eV was no longer detectable in the X-ray photoelectron spectrum of the nanocrystals, while a N 1s peak appeared at ~401.5 eV. This N 1s binding energy is consistent with values previously observed for hydrazines on GaAs[44] and Ru[45] surfaces.

No As oxide contaminants were observed even though the samples had been treated with water and acetone after exposure to the hydrazine. The observed As photoemission peak was resolved into two spin−orbit doublets, with the $3d_{5/2}$ components centered at 41.1 and 41.7 eV, respectively, having an area ratio of 1:2. Hence the surface of the hydrazine-exposed particles was even more As-rich than the surface of the Cl-terminated nanoparticles.

The Ga 3d spectrum of the hydrazine-exposed nanoparticles displayed two peaks, a larger bulk emission at 19.5 eV and a smaller component shifted to 20.1 eV. This latter binding energy is consistent with Ga_2O, although a contribution from nitrogen-bonded surface Ga atoms is also possible. The bulk-to-surface species intensity ratio was 4.2:1.

3.3.1.2. Infrared Spectroscopy. The IR spectra of the hydrazine-capped nanoparticles showed a significant amount of adsorbed water, which obscured observation of N−H stretching

(38) Surdu-Bob, C. C.; Saied, S. O.; Sullivan, J. L. *Appl. Surf. Sci.* **2001**, *183*, 126.
(39) Webb, L. J.; Nemanick, E. J.; Biteen, J. S.; Knapp, D. W.; Michalak, D. J.; Traub, M. C.; Chan, A. S. Y.; Brunschwig, B. S.; Lewis, N. S. *J. Phys. Chem. B* **2005**, *109*, 3930.
(40) Seah, M. P. Quantification of AES and XPS. In *Practical Surface Analysis*, 2nd ed.; Briggs, D., Seah, M. P., Eds.; John Wiley & Sons: Chichester, 1990; Vol. 1; p 201.
(41) Martin-Concepcion, A. I.; Yubero, F.; Espinos, J. P.; Tougaard, S. *Surf. Interface Anal.* **2004**, *36*, 788.
(42) Sanchez-Lopez, J. C.; Fernandez, A. *Surf. Interface Anal.* **1998**, *26*, 1016.
(43) Thurmond, C. D.; Schwartz, G. P.; Kammlott, G. W.; Schwartz, B. *J. Electrochem. Soc.* **1980**, *127*, 1366.
(44) Sun, Y. M.; Sloan, D. W.; McEllistrem, M.; Schwaner, A. L.; White, J. M. *J. Vac. Sci. Technol., A* **1995**, *13*, 1455.
(45) Truong, C. M.; Rodriguez, J. A.; Goodman, D. W. *J. Phys. Chem.* **1992**, *96*, 341.

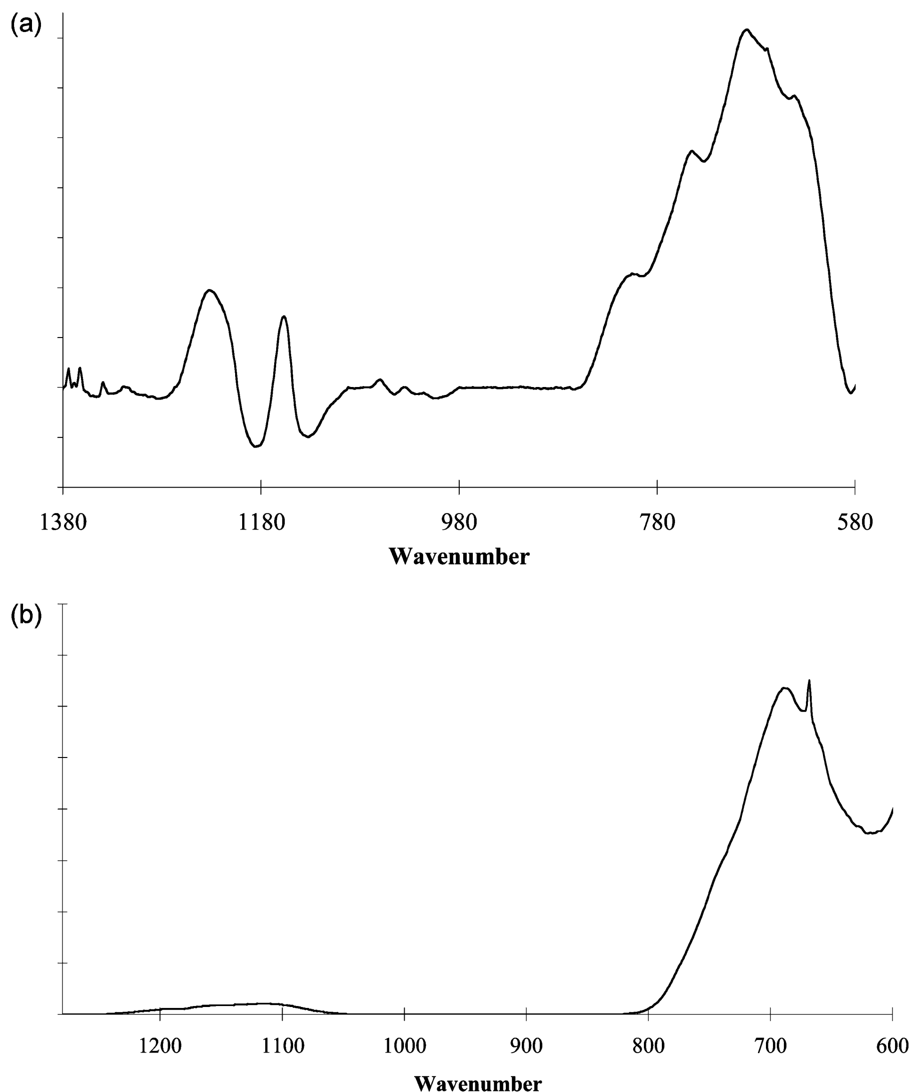

Figure 7. Diffuse reflectance infrared spectra of hydrazine-functionalized GaAs nanocrystals before (a) and after (b) annealing. Peak assignments are discussed in the text.

bands in the region between ~3200 and 3300 cm^{-1}. Reflectance bands of varying intensity were observed at 1225, 1155, 1090, 800, 737, 685, and 635 cm^{-1} (Figure 7a). Immediately after annealing, the IR spectrum of the particles was dominated by a single, broad reflectance peak at 685 cm^{-1} (Figure 7b). A small, very broad reflectance centered at ~1100 cm^{-1} was also observed. Some samples also included broad peaks at ~1210, 1150, 1090, 820, and 680 cm^{-1}.

Assignment of these bands is difficult due to disagreement on the energies of vibrational modes for both hydrazine and GaAs surfaces modified with nitrogen moieties. Previous reflectance IR studies of the nitridation of single-crystal GaAs surfaces with atomic nitrogen reported values of 1200 cm^{-1} and 1000 cm^{-1} for a Ga−N stretch and an As−N stretch, respectively.[46] A high-resolution electron energy loss spectroscopy (HREELS) study of hydrazine on GaAs(100)-c(8 × 2) assigned a loss feature at 1295 cm^{-1} to a Ga−NH_2 stretch,[47] while a similar study of ammonia on GaAs(100)-c(8 × 2) assigned loss features at 618 and 985 cm^{-1} to Ga−N stretching and Ga−NH_3 rocking modes, respectively.[48] For NH_3[49] and dimethyl hydrazine[44] on GaAs(100) (4 × 6), White et al. assigned an HREELS peak at 844 cm^{-1} to Ga−NH_x stretching.

Based on the spectra of the oxide-terminated particles, we assign the peak at 1225 cm^{-1} to Ga_2O and the peaks at 635 and 800 cm^{-1} to contamination from As_2O_3 in either the Claudetite or amorphous phase. It should also be noted that Ga−N vibrational modes have been observed in diffuse reflectance IR experiments on GaN powder[50] at 1230, 800, and 630 cm^{-1} and may not be readily distinguishable from the oxide peaks. To confirm this assignment, IR spectra of the particles were taken after several weeks of exposure to air. Consistent with the XPS results showing some oxide formation, the intensity of these peaks was greatly enhanced. Further, for unannealed samples with excess As at the surface, the spectrum of the air-exposed particles was dominated by the peak at 800 cm^{-1}, while this peak was much weaker for the annealed samples (vide infra). The peak at 737 cm^{-1} is near the value

(46) Yamauchi, Y.; Uwai, K.; Kobayashi, N. *Jpn. J. Appl. Phys. Part 2* **1996**, *35*, L80.
(47) Apen, E.; Gland, J. L. *Surf. Sci.* **1994**, *321*, 308.
(48) Apen, E.; Gland, J. L. *Surf. Sci.* **1994**, *321*, 301.
(49) Zhu, X. Y.; Wolf, M.; Huett, T.; White, J. M. *J. Chem. Phys.* **1992**, *97*, 5856.
(50) Centeno, M. A.; Delsarte, S.; Grange, P. *J. Phys. Chem. B* **1999**, *103*, 7214.

760 cm^{-1} observed for a shoulder in the Ga_2O_3 spectrum[35] and can thus be assigned to this species.

To help identify the peaks at 1155, 1090, and 685 cm^{-1}, the Cl-terminated GaAs nanoparticles were functionalized with a 35 wt % solution of N_2D_4 in D_2O. As with N_2H_4-treated particles, the relative intensity of the peaks varied significantly between the various N_2D_4-treated samples. However, the energies of the peaks in the spectrum were unchanged, with the exception of a new peak at 1970 cm^{-1}. This behavior suggests that these other peaks are due to either N-bonded surface species or are due to other oxide phases that could not be distinguished by XPS. Because the peak at 685 cm^{-1} is so dominant after annealing, it is unlikely to be related to surface As species. We assign this peak to Ga_2O_3, which has previously been observed at 680 cm^{-1}.[35,36] Peaks at 1080 and 1151 cm^{-1} have been observed during surface IR studies of GaAs(100) modified with Na_2S and have been assigned to S−O stretches,[51] although that assignment is clearly not applicable here. A broad peak at 1100 cm^{-1} has been observed for Claudetite As_2O_3[36] and can be correlated to observed peaks at 1090 and 1100 cm^{-1}. The peak at 1150 cm^{-1} does not correspond to any known gallium or arsenic oxide modes.

3.3.2. NaSH-Treated Samples. Treatment of the Cl-terminated GaAs nanoparticles with NaSH produced similar XPS behavior as that observed following treatment with hydrazine. Specifically, exposure to NaSH led to the disappearance of the Cl 2p peak and the appearance of a S 2p doublet, with the S $2p_{3/2}$ peak centered at 160 eV. Elemental As was still present in detectable amounts on the SH-exposed surfaces, although the contaminant-to-bulk ratio in the As 3d region was greatly reduced (1:5.3).

3.3.3. Annealed Surfaces. To remove the elemental As and As−N species from the nanocrystal surfaces, some hydrazine-exposed samples were annealed at 350 °C under vacuum. During the annealing process, black and pale yellow solids collected on the cold finger of the sublimator.

The photoelectron spectra of these samples showed that several significant changes were effected by the annealing step. The As 3d region was well-described by only a single doublet, corresponding to the bulk (Ga)As peak at 41.1 eV (Figure 8). A signal at ~44.7 eV was also visible, representing some As oxide contamination, but this peak was too small and broad for a reliable fit to be obtained. The Ga 3d region still contained a bulk peak at 19.3 eV, but the peak at 20.1 eV was replaced by a signal at 20.7 eV. The change in the Ga 3d spectra was accompanied by a shift in the binding energy of the N 1s peak from 401.5 to 398.3 eV (Figure 9), indicative of the reduction of surface-bound nitrogen. The observed N 1s peak energy is 1.2 eV higher in binding energy than the value of 397.1 eV reported for (Ga)N.[52] This peak is more consistent with the binding energy of 398.2 eV observed for $Ga_{(x+2)}N_{3x}O_{(3-3x)}$ formed during the dry oxidation of GaN.[53] In conjunction with the Ga 3d peak at 20.7 eV, the data therefore suggest that the annealing step led to the formation of a gallium oxynitride phase on the surface. Given the reported values of 398.5 eV for NH_x ($x = 1,2$) on GaAs[49] or 397.7 eV for imide on Ru(0001),[45] Ga-bound surface amide or imide species cannot be definitively ruled out, however. The observed binding energies of the As $3d_{5/2}$, Ga 3d, and N 1s peaks after etching, N_2H_4 treatment, and annealing, respectively, are summarized in Table 1. The bulk Ga to bulk As ratio was observed to be ~1:1, as expected for the core of the nanocrystals.

For a surface of terminal amides or imides, hydrogen atoms should be driven off at higher temperature to form a surface-capping layer of either terminal nitrides or cubic GaN. After annealing the hydrazine-terminated nanocrystals at 500 °C under

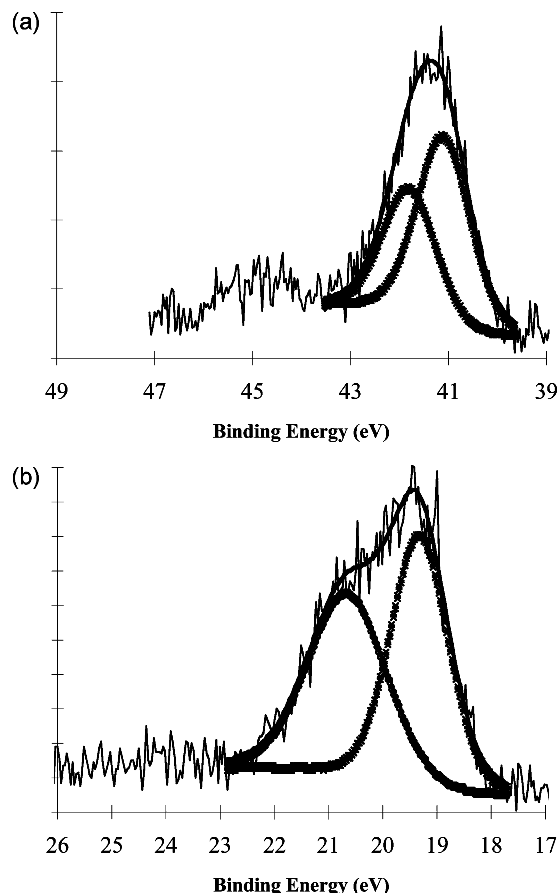

Figure 8. XPS spectra of N_2H_4-functionalized GaAs nanocrystals after annealing under vacuum at 350 °C. The As 3d spectrum (a) has been fit to a single doublet corresponding to bulk (Ga)As. A small amount of As oxide is also visible at higher binding energy. The Ga 3d spectrum (b) has been fit to two peaks, corresponding to bulk Ga(As) and Ga_2O_3.

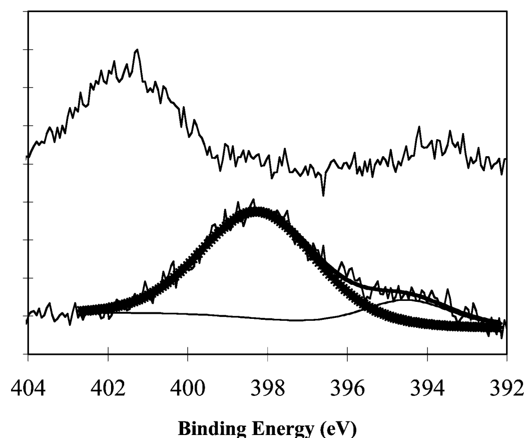

Figure 9. XPS data for the N 1s region of N_2H_4-functionalized GaAs nanocrystals before (upper) and after (lower) annealing. The peak at 394 eV is a Ga Auger line.

(51) Yota, J.; Burrows, V. A. *J. Vac. Sci. Technol., A* **1993**, *11*, 1083.
(52) Hedman, J.; Martensson, N. *Phys. Scr.* **1980**, *22*, 176.
(53) Wolter, S. D.; DeLucca, J. M.; Mohney, S. E.; Kern, R. S.; Kuo, C. P. *Thin Solid Films* **2000**, *371*, 153.

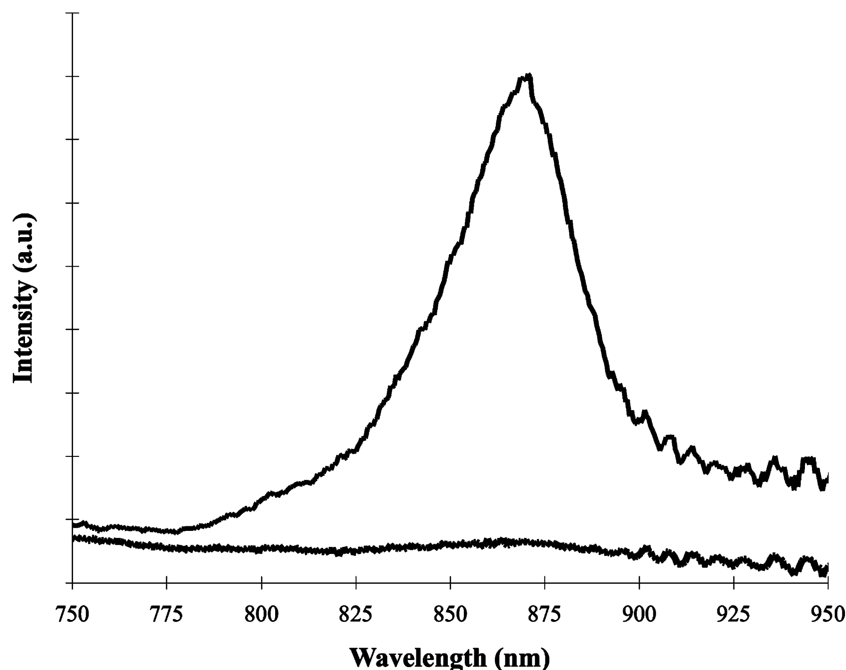

Figure 10. Steady-state photoluminescence intensity of N_2H_4 functionalized samples before (lower trace) and after (upper trace) annealing. No measurable signal was observed from oxide-terminated samples.

Table 1. Core Photoelectron Binding Energies (eV, Referenced to the (Ga)As $3d_{5/2}$ Peak at 41.1 eV)

photoelectron line	Cl-terminated GaAs nanocrystals	N_2H_4 treated, unannealed	N_2H_4 treated, annealed
As $3d_{5/2}$	41.1, 41.7	41.1, 41.7	41.1
Ga 3d	19.3, 20.1	19.5, 20.1	19.3, 20.7
N 1s		401.5	398.3

vacuum, they were no longer sufficiently conductive to perform XPS experiments without charge compensation from the electron flood gun. Spectra collected using the flood gun revealed a N 1s peak centered at 398.4 eV, i.e., virtually unchanged in energy from the peak observed following the lower temperature annealing step. This result is more consistent with the formation of a thicker oxynitride surface layer than the loss of hydrogen from amides or imides.

The annealed nanocrystals showed formation of both Ga and As oxides after 2 weeks in air. The N-capping layer was not stable in the original etching solution, and the photoelectron spectra of re-etched nanocrystals showed the disappearance of the N 1s signal and the reappearance of As^0.

3.3.4. Photoluminescence of Functionalized GaAs Nanocrystals. As the size of a semiconductor nanocrytal decreases below its excitonic Bohr radius, the band structure undergoes quantum confinement and the band gap of the nanocrystal increases.[32] Brus has calculated that GaAs ought to display bulk band gap behavior down to diameters of ~19 nm.[32] Based on the size measurements described above, a substantial majority of our nanocrystals were larger than this size, so their band edge PL should be dominated by emission at the bulk band gap energy, i.e., 1.43 eV (869 nm).

For particles dispersed on Si substrates, all of the samples examined displayed broad light scattering peaks centered between 650 and 700 nm. No photoluminescence was observed from the oxide-capped nanocrystals. Only a weak PL peak, centered at 868 nm, was observed for nanocrystals that had been etched and treated with either N_2H_4 or NaSH. In contrast, nanocrystals that had been capped with either of these reagents and additionally had been annealed displayed a peak at this wavelength that was more than 40 times more intense than the other samples, suggesting significant suppression of surface trap states (Figure 10). The PL intensity of these particles did not degrade even after several weeks in air, despite the fact the XPS revealed the formation of some surface oxides.

For particles dispersed in CH_3OH, photoluminescence was observed only from particles that had been N_2H_4-capped and annealed. However, when the GaAs nanoparticles were subsequently dispersed on Si, all but the as-prepared oxide capped particles photoluminesced to at least some extent. Therefore, we attribute this reduced PL signal in CH_3OH either to increased scattering or to a solution quenching process rather than chemical degradation by CH_3OH. The fact that the N_2H_4-treated and annealed particles still showed significant PL under these conditions makes them an especially promising candidate for photoelectrochemical applications.

4. Conclusions

Oxide-terminated GaAs nanocrystals have been chemically synthesized and etched to yield nanocrystals with Cl-terminated surfaces. These reactive surfaces have been used as platforms for further functionalization with hydrazine or sodium hydrosulfide. The surfaces of Cl-, hydrazine- and hydrosulfide-capped nanocrystals all contained significant amounts of As contaminants and only displayed very weak band-edge PL. Annealing the functionalized nanocrystals under vacuum removed the excess As and, in the case of the hydrazine-functionalized particles, led to decomposition of surface-bound N_2H_4 into a surface exhibiting XPS and IR data consistent with the formation of a capping gallium oxynitride layer. The band edge PL of the GaAs nanoparticles was strongly enhanced after this annealing step, confirming both that elemental As is an important electronic trap state for GaAs nanocrystals and that this

functionalization chemistry effectively reduces the density of surface-related carrier trap states.

Acknowledgment. We gratefully acknowledge the U.S. Department of Energy, Office of Basic Energy Sciences, for support of this work. We thank Dr. Carol Garland for assistance collecting TEM images. This research was carried out in part at the Molecular Materials Research Center in the Beckman Institute at Caltech.

JA076034P